

# Scaling and universality in transition to synchronous chaos with local-global interactions

Prashant M. Gade<sup>1,2</sup> and Chin-Kun Hu<sup>1,\*</sup>

<sup>1</sup>*Institute of Physics, Academia Sinica, Nankang, Taipei 11529, Taiwan*

<sup>2</sup>*Center for Modeling and Simulation, University of Pune, Pune, 411 007, India*

(Received 30 September 2004; revised manuscript received 13 December 2005; published 20 March 2006)

We study the coupled-map lattice model with both local and global couplings. We find necessary conditions for observing synchronous chaos and investigate the transition to synchronization as a dynamic phase transition. We discover that this transition, if continuous, shows scaling and universal behavior with the dynamic exponent  $z=2$ . We also define and illustrate an interesting quantity similar to persistence at critical point.

DOI: 10.1103/PhysRevE.73.036212

PACS number(s): 05.45.Ra, 05.45.Xt

## I. INTRODUCTION

Universality and scaling in critical many-body systems [1,2] can be considered to be one of the important scientific discoveries in statistical physics. This critical behavior is often able to distinguish between essential and not so essential details of the system. For example, the phase transitions in the Ising model and the percolation model have been investigated on various two-dimensional lattices (square, honeycomb, triangular, and random) and the same sets of critical exponents and finite-size scaling functions have been found for the Ising and percolation models [2], respectively. These ideas have been used in dynamical systems theory also. For example, it was established that all one-hump quadratic maps which undergo a period-doubling cascade have the same set of critical exponents [3]. Thus seemingly disparate models could have the same underlying dynamics. We can ask similar questions about nonequilibrium systems such as spatially extended dynamical systems and the stochastic models. In this work, we will try to see if one can draw parallels between phase transitions in these systems. In particular, we will be interested in similarity between the transition to directed percolation (DP) in stochastic systems [4] and the synchronization transition in spatially extended dynamical systems [5].

Here we will investigate a popular model of spatiotemporal dynamical systems, the coupled map lattice (CML), which was proposed by Kaneko simultaneously with Waller and Kapral in the 1980s [6,7]. It was then studied extensively by Kaneko and several others [7], and is now a prototype for a spatially extended dynamical system. It has been studied on various types of lattices. It has found applications in modeling problems as diverse as spiral formation to the stock market [8,9]. The criterion for transition to synchronization in CML in the thermodynamic limit is now well understood and is related to the presence of a gap in the eigenvalue spectrum of the connectivity matrix [5]. (Similar criterion is also applicable to continuous time systems such as coupled oscillators [10].) It seems that the system needs to have non-local (i.e., long-range) interactions, in order to achieve this gap in an eigenvalue spectrum in the thermodynamic limit.

Purely local couplings, *in any dimension*, cannot lead to a synchronous chaotic state [11,12] for an infinite array. In this sense, transition to synchronization as dynamic phase transition is rather unique since in many other systems, the transition for the mean-field case is in the same universality class as one observed for dimension  $d \geq d_c$ , where  $d_c$  is a critical dimension. On the other hand, transition to synchronous chaos exists only in the presence of long-range interactions and there can be no meaningful comparison with a finite-dimensional system.

There are several reasons that phenomenon of synchronous chaos in spatially extended systems has attracted much attention in the recent decade [5,10,13]. It has practical applications such as secure communication. Besides, there are physical grounds that make it necessary to investigate this problem. Physically, synchronous chaos does appear in systems such as the visual cortex [14]. We would like to note that the importance of nonlocal interactions in neurobiology is well acknowledged [15,16].

Since we are emphasizing the role of long-range interactions, it could be worthwhile to ask how prevalent such interactions are. In fact, there are several physical systems in which nonlocal or long-range interactions arise naturally. Recently, Tsallis proposed a thermodynamics to deal with these systems [17]. We should note that even if long-range interactions are not explicitly present in the system, they may be present in equations of simplified models. Integro-differential equations arise in various branches of science. As an example, we can consider a system in which some variables have faster time scale of evolution compared to others. In this case, if one writes down equations for slow variables alone, the fast variables could appear averaged out over entire system, thus giving a global contribution. Oxidation of CO on a Pt(110) surface is described by integro-differential equation in which both local and global terms play the role [18]. Integro-differential equations are also used to describe flame propagation [19]. Such nonlocal couplings can also be present in resultant equations when there is external forcing at length scale higher than the diffusion scale of the system. In center manifold reduction, such a term may arise and its contribution may not be negligible [20].

The problem of synchronization in spatially extended systems could be considered in two different ways. One is synchronization between two different replicas of the system that are coupled deterministically or stochastically. Another

\*Corresponding author. Email address: huck@phys.sinica.edu.tw

possibility is self-synchronization of all the elements of the same system. However, the synchronous state is an absorbing state in both cases, and thus the transitions in either case could be compared with the absorbing state phase transitions. We will be dealing with the transition to self-synchronization in coupled map lattices. Previous studies have dealt with stochastic synchronization between two spatially extended systems [21–23], which do not require the presence of non-local coupling [23]. There have been previous studies on the synchronization transition induced by common noise in spatially extended systems. The transition to synchronization of coupled cellular automata (CA) in the presence of a stochastic coupling mechanism has been investigated [22]. Grassberger [24] later showed that this transition in CA is in DP class. Baroni, Livi, and Torcini studied stochastic synchronization in CML, and conjectured that the transition to synchronization could be in DP class or Kardar-Parisi-Zhang class [25] depending on mechanism of information propagation [23]. Rolf, Bohr, and Jensen [26] studied spatiotemporal intermittency in specific maps that show spatiotemporal intermittency. It was discovered that the transition depends on whether the lattice is updated synchronously or asynchronously [27]. It was claimed that the transition is in DP class if the updates are *asynchronous*, while it could be in a different universality class when all sites are updated simultaneously. We will be dealing with exact synchronization in a coupled map lattice with purely deterministic rules without any stochastic component. Since the term “synchronous chaos” is undefined in the presence of asynchronous updates (though a synchronous fixed point is possible), we cannot have a valid comparison in this case. However, to our knowledge, transition to synchronization in CML, in the absence of noise (which requires the presence of nonlocal interactions) has not been investigated.

In this paper, we study the transition to synchronous chaos in the deterministic CML with local-global couplings and parallel update. We find necessary conditions for synchronous chaos. This helps us to know precisely the critical coupling strength for which synchronous chaos appears. For continuous transitions, we find that the approach of the system towards the synchronous chaotic state shows a universal behavior. On the other hand, transition to synchronous fixed point does depend on the nature of the map. We try to define certain order parameters and find critical exponents. The fact that we know the critical value of coupling parameter at the transition point is a big help in finding the exponents since a lot of computational time is usually spent in finding the critical point. Finding critical exponents exactly helps us to identify whether or not different systems are in the same universality class. We try to see if we can draw some parallel between stochastic systems and dynamical systems. We can never be exhaustive in numerical studies. However, for the cases we investigated, we find that if the transition is continuous, its critical behavior is similar to that of directed percolation.

This paper is organized as follows. In Sec. II, we define the model and state the condition for synchronization. In Sec. III, we define order parameter(s) for synchronous chaos and define critical exponents in a manner analogous to directed percolation. We then present numerical calculated results,

which show good scaling and universal behaviors with well-defined critical exponents. In Sec. IV, we consider the case of purely global coupling. In Sec. V, we briefly note that behavior of synchronous nonchaotic systems is very different. In Sec. VI, we define a quantity similar to persistence, which shows interesting scaling at critical point. In Sec. VII, we state the conclusions.

## II. THE MODEL

The CML with local-global couplings on a one-dimensional lattice of length  $N$  with periodic boundary conditions is defined as

$$\begin{aligned} x_i(t+1) = & (1 - \epsilon - \gamma)f(x_i(t)) + \frac{\epsilon}{2}[f(x_{i+1}(t)) + f(x_{i-1}(t))] \\ & + \frac{\gamma}{N} \sum_{j=1}^N f(x_j(t)). \end{aligned} \quad (1)$$

Here  $1 \leq i \leq N$ ,  $x_{N+1}(t) = x_1(t)$ , and  $x_0 = x_N$ . Parameters for local and global couplings are  $\epsilon$  and  $\gamma$ , respectively. When  $\epsilon=0$ , the model of Eq. (1) reduces to the globally coupled model studied by Kaneko [7]. Physically, the global field is often a bit delayed. However, we assume the delay to be small and ignore it. We have shown previously that a gap in the eigenvalue spectrum of the connectivity matrix leads to synchronous chaos [5]. We linearize the perturbation around the synchronized state and find that the eigenvalues in question are  $\lambda_l \exp(\lambda)$ , where  $\lambda$  is the Lyapunov exponent of the map  $f(x)$  and  $\lambda_l$  ( $1 \leq l \leq N$ ) are the  $N$  eigenvalues of the connectivity matrix [5]. They are given by  $\lambda_l = (1 - \epsilon - \gamma) + \epsilon \cos(2\pi l/N)$  for  $l=1, \dots, N-1$  and  $\lambda_N = 1$ . The  $\lambda_l$  ( $l \neq N$ ) are bounded between  $(1 - 2\epsilon - \gamma)$  and  $(1 - \gamma)$ . We assume that all couplings are positive. Thus, the quantity  $1 - \epsilon - \gamma \geq 0$ . Hence, we have  $0 \leq \epsilon \leq 1 - \gamma$ , which implies  $|\lambda_l| < 1 - \gamma$  (for  $l \neq N$ ). As  $N \rightarrow \infty$ , we note that  $\lambda_1 \rightarrow 1 - \gamma$  for  $\epsilon \neq 0$ . For  $\epsilon=0$ , we have an  $(N-1)$ -fold degenerate eigenvalue  $1 - \gamma$  and  $\lambda_N = 1$ . The condition for synchronized chaos is  $\lambda_l \exp(\lambda) < 1$  for  $l=1, 2, \dots, N-1$  and  $\lambda_N \exp(\lambda) = \exp(\lambda) > 1$ . Thus, for  $\gamma > \gamma_c = 1 - 1/\exp(\lambda)$ , synchronized chaos can be obtained in the thermodynamic limit for any value of  $\epsilon$ . (This is an exact threshold for any value of  $N$  for  $\epsilon=0$ , while this threshold is reached from below in the limit  $N \rightarrow \infty$  for  $\epsilon \neq 0$ .) Thus, the condition for synchronization in the limit  $N \rightarrow \infty$  is the same, irrespective of value of  $\epsilon$ . We also note that the threshold does not depend on details of the map, but just on the Lyapunov exponent of the map. For the extreme case  $\epsilon=0, \gamma=1$ , the synchronous state should always be stable. The result matches with the one for coupled maps with intermediate-range interactions in the limit of global coupling [5].

We note that the above condition is necessary but not sufficient for achieving synchronization. For example, for purely globally coupled system, symmetries and number of attractors in the system may make it impossible to reach a synchronous state [28].

We note that though local couplings do not change critical values, they reduce the symmetries of the system and hence

the number of attractors. Thus, local-global coupling makes the transition more robust. Furthermore, certain attractors such as clustered states are present only in globally coupled system *without* any local coupling. Thus, when synchronization is lost, new states that are formed are qualitatively different for purely-global and local-global coupling. When we discuss dynamics in detail, we will have an elaborate discussion of this difference between the models with local-global and purely-global coupling.

For  $f(x)$  of Eq. (1), we consider:

$$r(x) = \mu x(1-x), \quad 0 \leq \mu \leq 4, \quad 0 \leq x \leq 1; \quad (2)$$

$$g(x) = \begin{cases} ax, & \text{if } 0 \leq x < 0.5, \\ a(1-x), & \text{if } 0.5 < x \leq 1, \end{cases} \quad 0 \leq a \leq 2; \quad (3)$$

$$h(x) = \begin{cases} ax + 2 - a, & \text{if } 0 < x \leq 1 - 1/a, \\ a(1-x), & \text{if } 1 - 1/a < x \leq 1, \end{cases} \quad 1 < a < 2; \quad (4)$$

$$G(x) = \text{sgn}(x)g(|x|), \quad -1 \leq x \leq 1. \quad (5)$$

Functions  $r(x)$ ,  $g(x)$ , and  $h(x)$  are the well-known logistic map, tent map, and asymmetrical tent map, respectively. These functions map interval  $[0, 1]$  to itself and  $G(x)$  maps  $[-1, 1]$  onto itself. We note that under the evolution rule  $G(x)$ , the evolution of coupled maps is invariant under transformation  $x \rightarrow -x$ . The functions  $r(x)$  and  $g(x)$  are symmetric around the maximum, while  $h(x)$  is not. If we try to define maps over the extended interval  $[-1, 1]$  from  $r(x)$  and  $h(x)$  [say,  $R(x) = \text{sgn}(x)r(|x|)$ ], we do not get a continuous transition. The map  $h(x)$  becomes discontinuous if defined over  $[-1, 1]$  using  $h(-x) = -h(x)$ . Even slightly discontinuous maps lead to a discontinuous transition. However, it is not necessary that all continuous maps lead to continuous transitions. Symmetrized logistic maps also lead to discontinuous transitions. We must mention that, unfortunately, we have not been able to identify reasons as to when the transition is continuous and when it is not. In this paper, we will study only maps and parameter values at which a continuous transition to synchronization is obtained and study it as a dynamic phase transition [29].

The map  $G(x)$  is such that if all  $x_i(t)$  are positive (negative) for all sites  $i$  at any time  $t$ , they remain positive (negative) at all later times. The synchronized state is one such state. If the dynamics becomes synchronized, i.e.,  $x_i(t) = x^*(t)$  for all  $i$ , all the sites will be either positive or negative depending on the sign of  $x^*(t)$ . It is also guaranteed that they will stay so forever. Thus, synchronization will break the symmetry, making the values of all maps positive or negative forever. However, we do not find that this symmetry affects the transition. The reason could be that all sites having same sign is a much weaker condition than synchronization and does not even require nonlocal couplings [30]. Thus, this transition could occur at a different coupling than transition to synchronization, making the Ising symmetry irrelevant in transition to synchronization.

### III. SYNCHRONIZATION AS A DYNAMIC PHASE TRANSITION

To understand the behavior of approaching the synchronization, we define the following quantities:

$$d(N, t, \gamma_c - \gamma) = N^{-1} \sum_{i=1}^N |x_i(t) - x_{i+1}(t)|, \quad (6)$$

$$\rho(N, t, \gamma_c - \gamma) = N^{-1} \sum_{i=1}^N |x_i(t) - \langle x(t) \rangle|, \quad (7)$$

$$\sigma^2(N, t, \gamma_c - \gamma) = N^{-1} \sum_{i=1}^N (x_i(t) - \langle x(t) \rangle)^2, \quad (8)$$

where  $\langle x(t) \rangle = N^{-1} \sum_{i=1}^N x_i(t)$ . Obviously, all quantities above will be zero in the synchronous state and will have a positive value in the asynchronous state. Thus, they can be considered as some kind of “order parameter.” The quantities  $\rho(N, t, \gamma_c - \gamma)$  and  $\sigma^2(N, t, \gamma_c - \gamma)$  are, respectively, the first and second moments of absolute difference of variable values at various sites from the synchronous state at a given time  $t$ . The variable  $d(N, t, \gamma - \gamma_c)$  is different and looks at local fluctuations in the variables. This quantity is meaningful only in the presence of local couplings and shows a non-trivial behavior. In the language of spin systems, this quantity measures number of domain walls or kink density.

All the above quantities decay as a power law at  $\gamma = \gamma_c$  and  $N \rightarrow \infty$ . There are departures from this behavior at finite  $N$  and for  $\gamma \neq \gamma_c$ . We define  $\alpha_1$ ,  $\alpha_2$ , and  $\alpha_3$  as  $d(\infty, t, 0) \sim t^{-\alpha_1}$ ,  $\rho(\infty, t, 0) \sim t^{-\alpha_2}$ , and  $\sigma^2(\infty, t, 0) \sim t^{-\alpha_3}$ , respectively. In directed percolation, there is invariance under time reversal. Thus, the density of active sites at time  $t$  and probability of survival of a cluster starting from single site until time  $t$ , are equivalent [4]. However, we feel that order parameters defined above are more similar to fraction of active sites in directed percolation. Hence, we have chosen the symbol  $\alpha$  for the decay rate.

The quantity  $d(t)$  quantifies the difference between nearby sites. *We note that the coupling is not purely global and it makes significant differences in the dynamical behavior.* For purely global coupling, it is possible to have clustered states. We can have a group of sites  $i_1, i_2, \dots, i_k$  such that  $x_{i_1}(t) = x_{i_2}(t) = \dots = x_{i_k}(t)$  at all times. This state could be stable; i.e., it could be reached from several initial conditions. We note that if one introduces local coupling, this state does not even exist. Even if we start the system in an initial condition where two sites have the same variable value, they will not have the same value at the next time instant. The reason is that they see different local neighborhood and it affects them. For purely global coupling, the cluster state takes over when the synchronous state loses stability [31]. In the presence of local coupling, one cannot have a transition to the cluster state. Thus, the transitions in systems with  $\epsilon = 0$  and  $\epsilon \neq 0$  are expected to be qualitatively different from the viewpoint of dynamics.

We discuss the map  $G(x)$  in detail. Here the Lyapunov exponent of synchronized state is  $\log(a)$  at any time step.

The finite time Lyapunov exponent has zero variance and complications due to slow convergence of the Lyapunov exponent (often slower than the time scale in question) does not affect the convergence of the results. We have also studied logistic map at  $\mu=4$ , where the Lyapunov exponent is exactly known. We also use higher iterates of the map, i.e.,  $h^n(x)$  as a mapping function so that we can have larger Lyapunov exponent  $n \log(\lambda)$ , where  $\log(\lambda)$  is the Lyapunov exponent of  $h(x)$ . Thus, we can change the Lyapunov exponent of the map from near zero to arbitrarily large values.

For a finite system or when the global coupling is not exactly equal to the critical value, we find a departure from the power-law behavior at certain time  $t_c$ , which is a function of system size  $N$  and  $\gamma_c - \gamma$ . Let us first consider a case at which  $\gamma = \gamma_c$ . Here we expect the  $t_c \propto N^z$  for  $z > 0$  since for bigger and bigger system sizes, departure will be observed at longer times. The value of order parameter [say  $\sigma^2(N, t, 0)$ ] at the critical time  $t_c$  will be  $t_c^{-\alpha_3} \sim N^{-z\alpha_3}$  since  $\sigma^2(N, t, 0)$  decays as a power law until  $t_c$ . Now if a simple scaling holds, we can expect  $\sigma^2(N, t, 0)$  scaled by  $N^{-z\alpha_3}$  should be an universal function of scaled time  $t/t_c$ . In other words, we propose that

$$d(N, t, 0) = N^{-z\alpha_1} f(t/N^z), \quad (9)$$

$$\rho(N, t, 0) = N^{-z\alpha_2} f(t/N^z), \quad (10)$$

$$\sigma^2(N, t, 0) = N^{-z\alpha_3} f(t/N^z). \quad (11)$$

We observe that above scaling indeed holds beautifully for continuous transitions. However, before discussing finite-size scaling we discuss raw data briefly. We illustrate the behavior of scaling parameters for the map  $G(x)$  for various values of  $a$ . For this map,  $\lambda = \log(a)$  and  $\gamma_c = 1 - 1/a$ . We show behavior of variance  $\sigma^2(N, t, 0)$  as a function of time in Fig. 1 for different values of  $a$ ; i.e.,  $a = 1.01, 1.1, 1.3$ , and  $2$ . We find that for smaller values of  $a$ , variance decays as  $1/\sqrt{t}$  initially. For larger and larger values of  $\lambda$  the asymptotic behavior is more apparent. We note that the quantities  $\rho(N, t, 0)$  and  $d(N, t, 0)$  also show similar departure at short times, for smaller values of  $\lambda$ . The  $1/\sqrt{t}$  behavior is followed by a sharp drop in the value of variance at  $T_0(a)$ . The variance decays as  $1/t^2$  thereafter followed by an exponential contraction to the synchronous state at  $t > T_c(N)$ . We first investigate behavior at large values of  $\lambda$ . To get the asymptotic behavior clearly, we simulate the system at a large value of Lyapunov exponent and use  $f(x) = G^n(x)$  with  $a = 1.99999$ ,  $n = 3$ , and  $\lambda = 3 \log(a)$ . We simulate system at  $\epsilon = 0.1$  for various lattice sizes and plot  $\sigma^2(N, t, 0)$  as a function  $t$  for various values of  $N$  in Fig. 2(a). Taking values of  $z = 2$  and  $\alpha_3 = 2$ , we get an excellent data collapse for  $\sigma^2(N, t, 0)$  as shown in Fig. 2(b). Similar finite-size scaling for  $d(N, t, 0)$  and  $\rho(N, t, 0)$  yields  $\alpha_1 = 3/2$  and  $\alpha_2 = 1$ . Dynamic exponent  $z = 2$  for all the cases as long as  $\epsilon \neq 0$ .

Even for smaller values of Lyapunov exponent, the asymptotic behavior remains the same. We plot  $\sigma^2(N, t, 0)$  as a function of  $t$  for various values of  $N$  at  $a = \exp(\lambda) = 1.1$ ,  $\epsilon = 0.1$  in Fig. 3(a). We observe the same scaling function as in Fig. 2(b) gives an excellent scaling collapse at longer

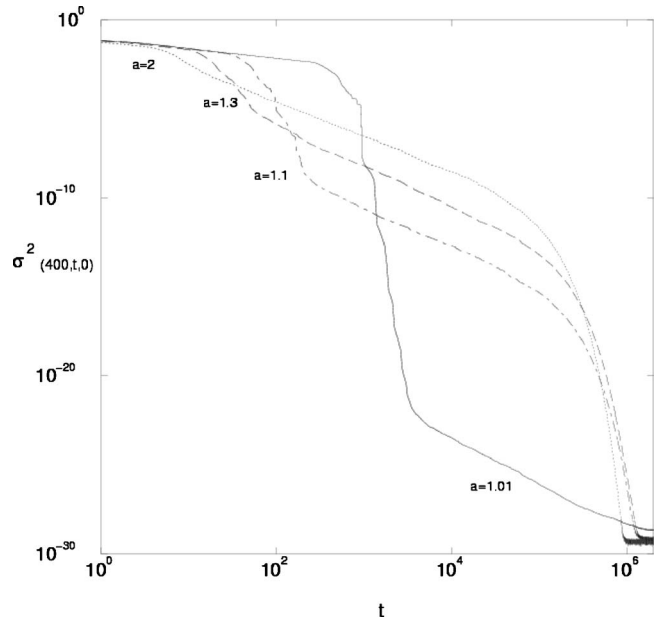


FIG. 1. The quantity  $\sigma^2(400, t, 0)$  for map  $f(x) = G(x)$  with  $\epsilon = 0.1$  and  $a = 1.01, 1.1, 1.3$ , and  $2$ . We average over 5000 configurations.

times shown in Fig. 3(b). However, behavior at short times is indeed affected for smaller Lyapunov exponent.

Now let us analyze the short-term behavior. In Sec. V, we show that  $(1/\sqrt{t})$  decay is expected in purely linear systems. We also note that the tent map for the parameter  $a \rightarrow 1$  is very close to a linear system. For a system with smaller Lyapunov exponent, longer time is required before the distance between closely trajectories is of the order of system size and they fold back. When this folding actually occurs, the system starts showing behavior expected in chaotic systems in general. Thus, we expect  $T_0(a) \propto 1/\lambda$ , so that for larger values of  $a$  (i.e.,  $\lambda$ ),  $T_0(a) \rightarrow 0$  and the long-term behavior becomes very clear.

To investigate the early behavior, we simulate the system for  $\epsilon = 0$  so that finite-size effects do not interfere with the analysis. In Fig. 4(a), the quantity  $\sigma^2(20, t, 0)$  is plotted as a function of time for map  $f(x) = G(x)$ , for  $\epsilon = 0$  and  $a = 1.05, 1.2, 1.5$ , and  $1.99$ . We plot the same quantity as a function of  $\lambda t$  in Fig. 4(b) and find that the drop occurs at approximately the same value of  $\lambda t$ . Thus, we can infer that the time  $T_0(a)$  at which there is departure from initial  $1/\sqrt{t}$  behavior scales as  $1/\lambda$  for the map  $G(x)$ . This is what we expected from the argument given in the previous paragraph.

We believe that  $z = 2$  for  $\epsilon \neq 0$  is related to the fact that true value of global coupling required for synchronization for any finite  $N$  is slightly lower than one required for an infinite system. The critical value needed for synchronization at finite  $N$ ,  $\gamma_c(N)$  differs from  $\gamma_c(\infty)$  by  $\epsilon[1 - \cos(2\pi/N)] \sim \epsilon/N^2$ . If we assume that the critical saturation time scales inversely with the difference of the value of  $\gamma$  from critical value, it follows that  $z = 2$ . Let us test this hypothesis about critical saturation time by investigating system for  $\gamma_c - \gamma \neq 0$ . We expect  $\sigma^2(\infty, t, \eta) \sim \eta^{\beta_3} g(t\eta)$ . [If saturation time  $t_c$  scales as  $\eta^{-1}$ , the width at saturation time is

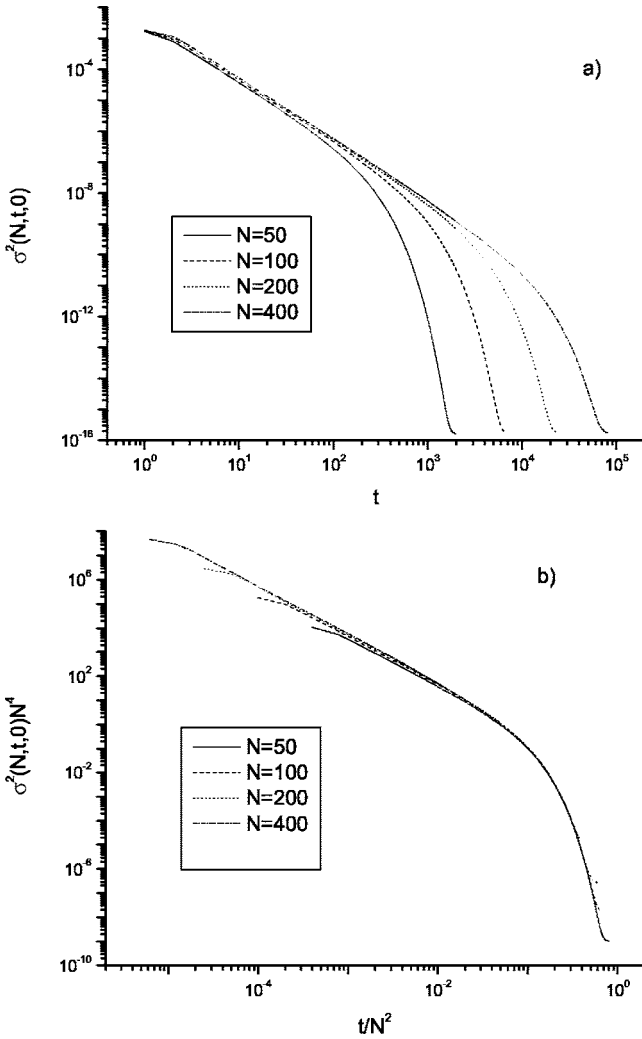


FIG. 2. (a) The quantity  $\sigma^2(N, t, 0)$  is plotted as a function of  $t$  for map  $f(x)=G^3(x)$  with  $a=1.999\ 99$  and  $\epsilon=0.1$  for various lattice sizes  $N$ . Averaging is done over  $10^4$  configurations. (b) The quantity  $\sigma^2(N, t, 0)N^4$  is plotted as a function of  $t/N^2$ .

$t_c^{-\alpha_3} \sim \eta^{\alpha_3}$ . We do find that  $\sigma^2(\infty, \infty, \eta) \propto \eta^{\beta_3}$  with  $\beta_3=\alpha_3$ .] Now, if we scale the width by saturation width and time in units of saturation time, we should get a scaling collapse. For  $f(x)=G^3(x)$  at  $a=1.999\ 99$  and for  $N=10^4$ , we simulated the CML for various values of  $\eta$ , and the results are shown in Fig. 5(a). (We simulate for large  $N$  so that finite size effects do not interfere with the results.) Now we plot  $\sigma^2(10^4, t, \eta)/\eta^2$  as a function of  $t/(1/\eta)=t\eta$ , and we get excellent scaling collapse in Fig. 5(b). This implies that  $\beta_3=2$ , which is the same as  $\alpha_3$  for this system. We can define  $\beta_1$  and  $\beta_2$  in a similar manner; i.e.,  $d(\infty, \infty, \eta) \propto \eta^{\beta_1}$  and  $\rho(\infty, \infty, \eta) \propto \eta^{\beta_2}$ .

As illustrated in various figures above, the time required for synchronization at  $\gamma=\gamma_c$  or the time in which the order parameter saturates to a nonzero value for  $\gamma<\gamma_c$  depends on value of  $N$  and of  $\gamma_c-\gamma$ . Using an argument similar to one used above, we expect that  $\beta_i=\alpha_i$ ,  $i=1, 2, 3$ . We have already demonstrated this for  $\sigma^2(N, t, \gamma_c-\gamma)$ . It is also true for other two order parameters. We have verified that  $\alpha_2=\beta_2=1$  by simulating system for various lattice sizes and various values

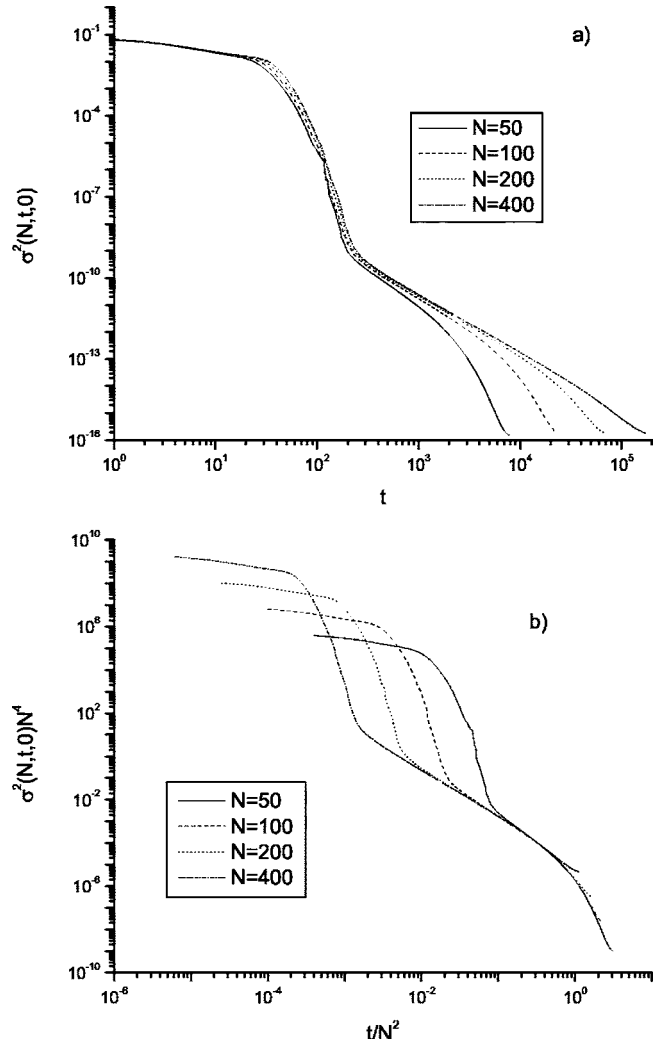


FIG. 3. (a)  $\sigma^2(N, t, 0)$  for various lattice sizes for  $f(x)=G(x)$  with  $a=1.1$  and  $\epsilon=0.1$ . Averaging is done over  $10^4$  configurations. (b) The quantity  $\sigma^2(N, t, 0)N^4$  is plotted as a function of  $t/N^2$ . For large  $t/N^2$ , we see a good data collapse at later times.

of  $\gamma$ . We note that  $\rho(N, t, \gamma_c-\gamma)$  and  $\sigma^2(N, t, \gamma_c-\gamma)$  are related order parameters. They are the mean and the variance of the probability distribution  $K(w)$  of the quantity  $w=|v|$ , where  $v_i=x_i(t)-\langle x(t) \rangle$ . Since the distribution at each site is expected to be the same, we drop the site index and average over all sites. In Fig. 6(a), we plot  $K(w)$  at various times. We use the logistic map with  $f(x)=g(x)$ ,  $\mu=4$ ,  $N=400$ ,  $\epsilon=0.1$ ,  $\gamma=\gamma_c$ , and average over  $10^4$  configurations. We can see that the raw data have an initial power-law decay followed by an exponential. We postulate that probability  $K(w)$  to be a gamma distribution, i.e.,  $K(w)=\Lambda^r w^{r-1} \exp(-\Lambda w)/\Gamma(r)$ , where  $\Lambda=t$ . It follows that  $K(w)/\Lambda=(\Lambda w)^{r-1} \exp(-\Lambda w)/\Gamma(r)$ . If the ansatz is truly satisfied, we should observe a scaling collapse by plotting  $K(w)/\Lambda=K(w)/t$  as a function of  $\Lambda w=wt$ . This collapse is demonstrated in Fig. 6(b). For the gamma functions, it is known that the mean goes as  $1/\Lambda=1/t$  and variance goes as  $1/\Lambda^2=1/t^2$ . Hence, we have  $\alpha_2=1$  and  $\alpha_3=2$ . It is interesting that the distribution of difference variables takes this simple form for different systems when they are near the critical point.

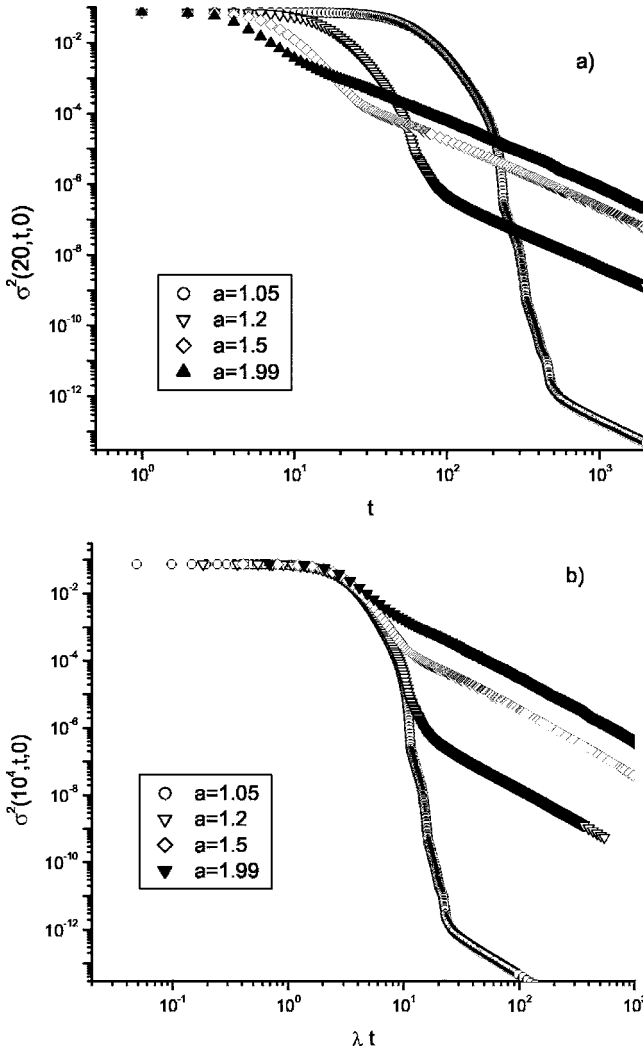


FIG. 4. (a) The quantity  $\sigma^2(20, t, 0)$  is plotted as a function of time for map  $f(x)=G(x)$ , for  $\epsilon=0$  and  $a=1.05, 1.2, 1.5$ , and  $1.99$ . Averaging is done over 8000 configurations. (b) The same quantity as above is plotted as a function of  $\lambda t$ . We can infer that the time at which there is departure from initial  $1/\sqrt{t}$  behavior in tent map scales as  $1/\lambda$ .

Now we discuss  $d(N, t, \gamma_c - \gamma)$  in detail since it looks at local details of the system. We note that we can write  $x_i(t) - x_{i+1}(t)$  as  $[x_i(t) - \langle x(t) \rangle] - [x_{i+1}(t) - \langle x(t) \rangle] = v_i(t) - v_{i+1}(t)$ . The probability distribution  $R(v)$  for  $[x_i(t) - \langle x(t) \rangle]$  is symmetric around zero and is related to probability distribution  $K(w)$  of the absolute value of this variable. In particular,  $R(v) = R(-v) = K(|v|)/2$ . Thus, if the variables  $x_i(t)$  and  $x_{i+1}(t)$  were independent, we could get information about this order parameter by performing convolution of the probability distribution  $R(v)$ . However, we do not need an entire probability distribution of  $|x_i(t) - x_{i+1}(t)|$ . We are interested only in dependence of its mean value on  $t$ . Hence, we employ a simpler approach. Let us consider a quantity  $U(N, t, \gamma_c - \gamma) = \sum_{i=1}^N [x_i(t) - x_{i+1}(t)]^2$ . Now  $U(N, t, \gamma_c - \gamma) = \sum_{i=1}^N [v_i(t) - v_{i+1}(t)]^2$ . We know the variance of quantity  $v_i(t)$  or  $v_{i+1}(t)$ , which is given by  $\sigma^2(N, t, \gamma_c - \gamma)$ , decays as  $1/t^2$ . We also know that for independent variables  $X$  and  $Y$ ,

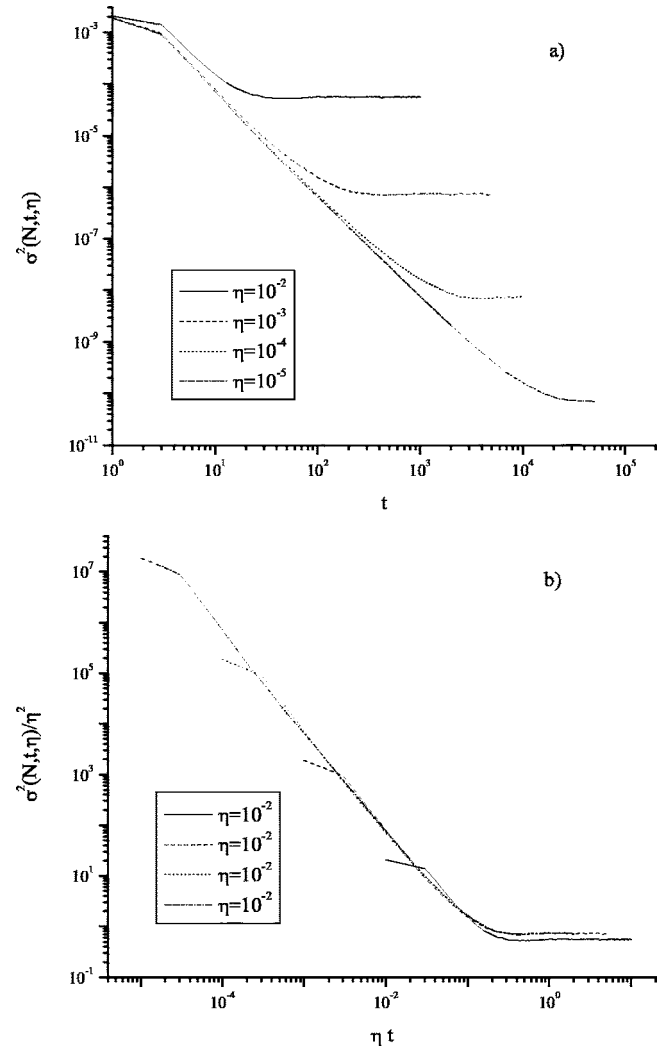


FIG. 5. (a) The quantity  $\sigma^2(N, t, \eta)$  is plotted as a function of  $t$  for various values of  $\eta$ . We have taken  $N=10^4$ ,  $f(x)=G^3(x)$  with  $a=1.99999$  and  $\epsilon=0.1$ . Averaging is done over 4000 configurations. (b) The quantity  $\sigma^2(N, t, \eta)/\eta^2$  is plotted as a function of  $\eta t$ .

$\text{Var}(aX+bY)=a^2 \text{Var}(X)+b^2 \text{Var}(Y)$ , and thus the quantity  $U(N, t, \gamma_c - \gamma)$  is expected to decay as  $1/t^2$  if  $v_i(t)$  and  $v_{i+1}(t)$  were independent. (We assume that they are identically distributed.) Thus,  $\sqrt{U(N, t, \gamma_c - \gamma)}$  behaves as  $1/t$  for the case of independent variables. Now, what is the relation between  $d(N, t, \gamma_c - \gamma)$  and  $\sqrt{U(N, t, \gamma_c - \gamma)}$ ? While one is the sum norm for the variables  $o_i=(x_i - x_{i+1})$ , the other is the Euclidean norm for the same set of variables. It can be shown that the sum norm can be bounded from above and below by constant multiple the Euclidean norm [32]. These constants do not change in time. This implies that  $d(N, t, \gamma_c - \gamma)$  is bounded between by  $A\sqrt{U(N, t, \gamma_c - \gamma)}$  and  $B\sqrt{U(N, t, \gamma_c - \gamma)}$ , where  $A$  and  $B$  are positive constants. Given that  $\sqrt{U(N, t, \gamma_c - \gamma)}$  goes as  $1/t$ ,  $d(N, t, \gamma_c - \gamma)$  cannot decay faster or slower than  $1/t$ . Thus, we expect it to decay as  $1/t$  implying  $\alpha_1=1$ . This expectation (and underlying assumption that nearby sites are independent for all practical purposes) is indeed fulfilled for the case  $\epsilon=0$ .

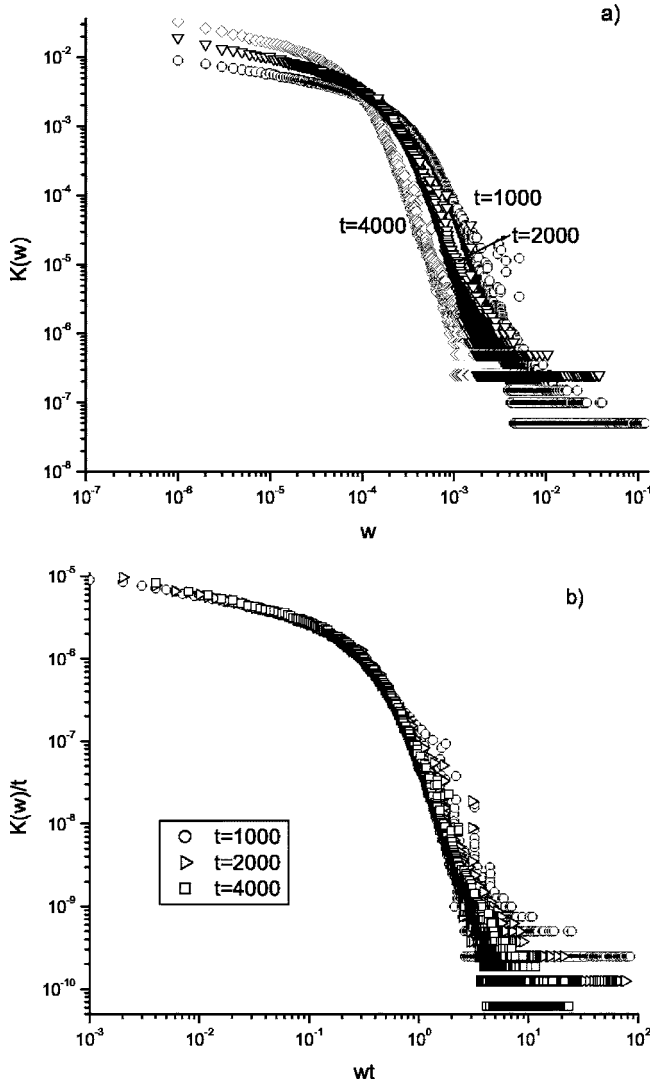


FIG. 6. (a) The probability distribution  $K(w)$  of  $w$ , where  $w = |x_i(t) - \langle x(t) \rangle|$  is plotted for various times. We use logistic map as  $f(x)$  and parameters used are  $\mu=4$ ,  $N=400$ ,  $\epsilon=0.1$ , and  $\gamma=\gamma_c$ . Averaging is done over  $10^4$  configurations. (b) For the data in (a), we plot  $K(w)/t$  as a function of  $wt$ . The collapse clearly indicates that the  $K(w)$  is a gamma distribution.

However, in presence of nearest-neighbor couplings, the values at nearby sites are highly correlated and we observe a different behavior. We use  $f(x)=G(x)$  with  $a=1.9999$ ,  $\lambda=\log(a)$ , and  $\epsilon=0.1$ . In Fig. 7(a), we show the behavior of  $d(N,t,0)$  as a function of  $t$  for various values of  $N$ . For  $\alpha_1=3/2$  and  $z=2$ , we observe an excellent scaling collapse that is displayed in Fig. 7(b). To find the value of  $\beta_1$ , we simulate the system at values of global coupling strengths that are slightly lower than critical coupling strength. We have shown  $d(N,t,\eta)$  for  $N=10^4$  and various values of  $\eta$  in Fig. 7(c). Using the scaling function defined above, we observe an excellent scaling collapse for  $\beta_1=3/2$  and  $z=2$  [see Fig. 7(d)]. The fact that  $\alpha_1 \neq \alpha_2$  shows that the short-range fluctuations in the variable values decay in a manner different than their fluctuations from the global average. The investigations of short-range fluctuations makes sense only in

the presence of local couplings. In the next section, we show that this behavior changes completely for  $\epsilon=0$ , showing the subtle effects that the presence of local coupling produces, though it does not change the critical coupling strength in the thermodynamic limit.

#### IV. PURELY GLOBAL COUPLING

As mentioned above, one obvious difference between the cases  $\epsilon=0$  and  $\epsilon \neq 0$  is the possibility of clustered states in desynchronized regime for  $\epsilon=0$ . We would like to mention one more difference in the dynamics of these two cases by looking at eigenvalue distribution at the critical point when the synchronized state becomes marginally unstable. For the case  $\epsilon=0$ , the eigenvalue spectrum is  $(N-1)$ -fold degenerate and all eigenmodes become marginally stable for  $\gamma=\gamma_c$ . On the other hand, for  $\epsilon \neq 0$ , the long-wavelength eigenmodes corresponding to  $l=1$  and  $l=N-1$  are unstable modes when synchronization is just lost. Thus for  $\epsilon=0$ , all the modes become marginally stable at the same parameter value leading to desynchronization for  $\gamma < \gamma_c$ . On the other hand, for  $\epsilon \neq 0$ , only long-wavelength modes become unstable when synchronization is lost. Thus, we do expect and observe certain dynamical differences, in the cases of purely global coupling, and when one has local as well as global coupling.

Setting the nearest-neighbor coupling to zero ( $\epsilon=0$ ), our system reduces to that with purely global coupling. In this case, we observe that  $z=0$  and do not really see any dependence on finite size. If we simulate the system at  $\gamma=\gamma_c$ , we observe excellent power laws for very long time. Reduction of  $z$  for nonlocal couplings is not surprising. For example, Mukherji and Bhattacharjee [33] studied the KPZ equation with nonlocal interactions and found reduction in dynamical exponent  $z$ . Since we are trying to make a comparison with directed percolation, we also note that directed percolation in the presence of nonlocal couplings was studied by Hinrichsen and Howard [34]. In the limit of coupling that decays as  $1/r$  in one dimension, they found  $\beta=\alpha=1$  and  $z=0$ . These values are the same as those for the order parameter  $\rho(N,t, \gamma-\gamma_c)$ . Since  $z$  is already reduced to zero when couplings decay as  $1/r$ , we expect it to be zero for the case of purely global coupling. (We also note that for Ising model, it is known that the mean-field theory is exact for ferromagnetic interactions that decay as  $1/r^\alpha$  for  $\alpha \leq d$  [35].) In this work, we have only studied the nonlocal coupling in the form of a global field. However, some researchers have considered fields that decay with distance and chaotic synchronization is observed in one dimension only when couplings decay more slowly than  $1/r$  [12]. Thus, we feel that it is a valid comparison. As mentioned above, if  $\rho(N,t, \gamma_c-\gamma)$  is considered an order parameter similar to active sites in directed percolation, we have exponents that are the same as anomalous directed percolation in the limit of global coupling. For the mean-field limit of directed percolation, the exponents are  $\beta=\alpha=1$  and  $z=2$ , which are the same as ones observed for  $\epsilon \neq 0$  in the CML studied in this paper.

As mentioned before, the behavior of quantity  $d(N,t,0)$  changes completely in the absence of local coupling. The quantity  $d(N,t,0)$ , which measures the absolute difference

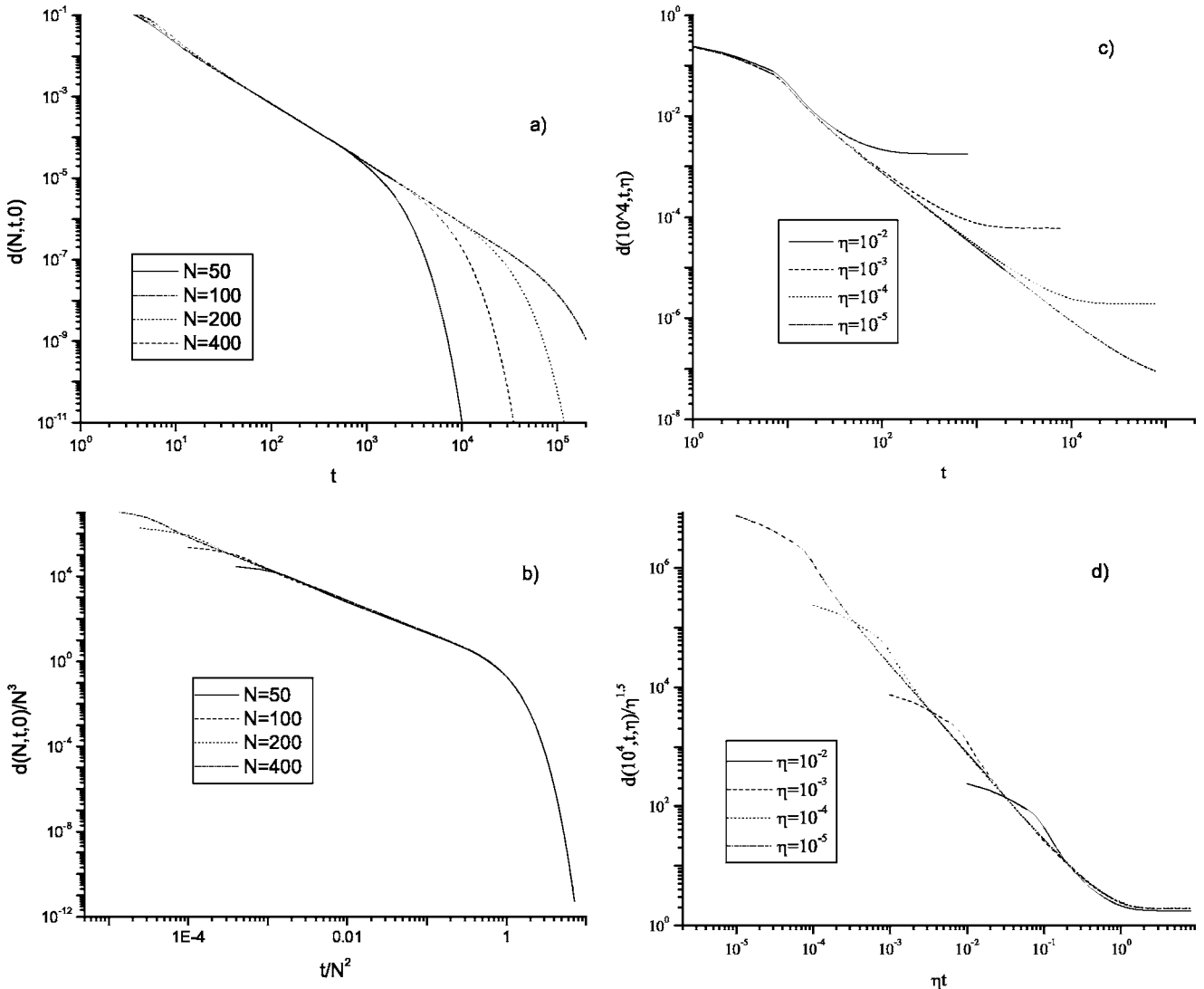


FIG. 7. (a) We show the behavior of  $d(N, t, 0)$  as a function of  $t$  for various values of  $N$ . We use  $f(x)=G(x)$  with  $a=1.9999$  and  $\epsilon=0.1$ . We average over 8000 configurations. (b) We plot  $d(N, t, 0)/N^3$  as a function of  $t/N^2$  for the above data. The scaling collapse indicates that  $\alpha_1=3/2$ . (c) Here we show  $d(N, t, \eta)$  for  $N=10^4$  and various values of  $\eta$ . As in (a), we use  $f(x)=G(x)$  with  $a=1.9999$  and  $\epsilon=0.1$ . We average over 8000 configurations. (d) The quantity  $d(N, t, \eta)/\eta^{3/2}$  is plotted as a function of  $\eta t$ . The collapse indicates that  $\beta_1=3/2$  as well.

between the nearest neighbors, is not a meaningful quantity in the absence of local coupling since “neighbors” become undefined in that case. The hypothesis of independence between nearby sites becomes more reasonable if there is no coupling between nearby sites and the  $1/t$  decay that we expected by assuming nearby sites to be independent is expected to hold for  $\epsilon=0$ . Thus,  $\alpha_1=1$  for purely global coupling and  $\frac{3}{2}$  local-global coupling. To demonstrate this fact, for the local-global coupling system, we define a quantity,  $d_k(N, t, \eta)=\sum_{i=1}^N |x_i(t)-x_{i+k}(t)|$ . We note that  $d_1(N, t, \eta)=d(N, t, \eta)$ . We observe that for large  $k$ ,  $d_k(N, t, 0)$  decays with exponent  $1/t$  even for local-global coupling. We show the behavior of  $d(N, t, 0)$  and  $d_{500}(N, t, 0)$  as a function of time in Fig. 8. We use  $f(x)=g(x)$ ,  $a=2$  and average over 5000 configurations. There is a clear difference in the behavior of  $d(N, t, 0)$  and  $d_{500}(N, t, 0)$ . Thus, the difference between points that are close decreases with a different exponent than the difference between far-off points for the local-

global coupling. To summarize, we can say that there are some major differences in critical behaviors for local-global coupling and purely-global coupling. There is an anomalous behavior at short range in local-global coupling and the dynamic exponents  $z$  are 2 and 0, respectively, for local-global and purely-global couplings.

## V. SYNCHRONIZATION OF NONCHAOTIC SYSTEMS

Now let us study the behavior of this system without any nonlinearity; i.e., consider the marginal case  $f(x)=x$ , for which  $\gamma_c(\infty)=0$  for global coupling. We look at evolution of the system at this critical value. For  $\epsilon=0$ , system is simply an identity mapping and roughness does not change in time. The system for  $\epsilon \neq 0$  is linear and could be solved by Fourier methods. We find out the leading behavior for the case  $\epsilon=1$ . Roughness is the sum of powers in Fourier modes other than the synchronized mode. Assuming the initial distribu-

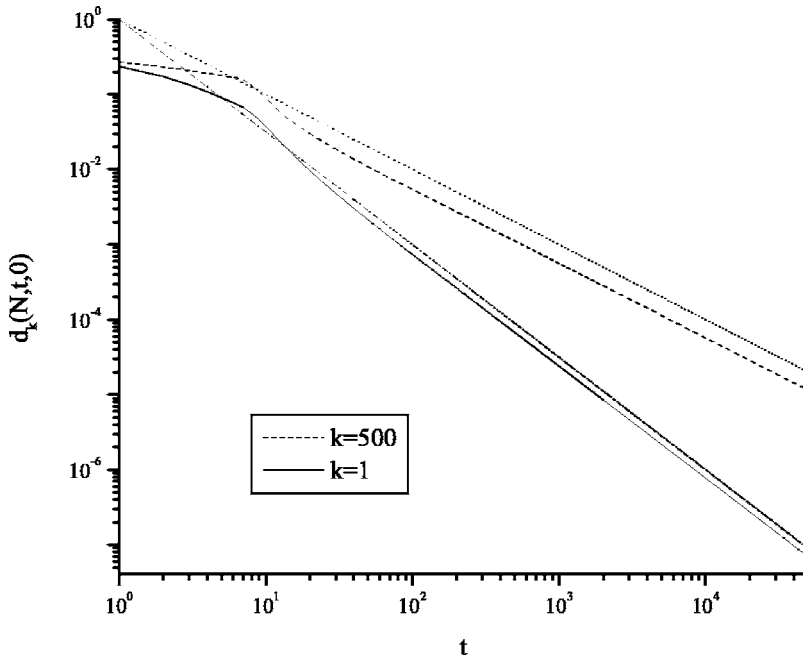


FIG. 8. For a local-global coupling system, the quantities  $d_1(10^4, t, 0)$  and  $d_{500}(10^4, t, 0)$  are plotted as a function of  $t$ . [Since  $d_k(N, t, \eta) = \sum_{i=1}^N |x_i(t) - x_{i+k}(t)|$ ,  $d_1(N, t, 0) = d(N, t, 0)$ .] We use  $f(x) = g(x)$ ,  $a = 2$ , and average over 5000 configurations. Lines  $1/t$  and  $1/t^{1.5}$  are also drawn as a guide to the eye.

tion to be random, we find that for  $\epsilon=1$ , roughness  $\sigma^2(N, t, 0) \sim \sum_{i=1}^{N-1} \cos^{2t}(2\pi i/N)$  [since each mode decays as  $\cos(2\pi i/N)$  and we assume that each mode had equal power in initial conditions]. For a large  $N$ , we can approximate the sum by an integral that has value  $2\pi[(2t-1)!!/(2t)!!] = 2\pi[2t!/(2t!)^2] = 2\pi 2^{-2}[2t!/(t!)^2]$ . To the first order,  $n! \sim \sqrt{2\pi n(n/e)^n}$ , which implies that roughness should decay as  $1/\sqrt{t}$ . Thus, the value of  $\alpha_3$  is  $1/2$ . We verify this behavior numerically. We find that  $\alpha_1=3/4$  and  $\alpha_2=1/4$ . Similar behavior is obtained for other values of  $\epsilon$ . The average time required for synchronization scales as  $1/L^2$  and we can obtain nice scaling. However, in presence of global coupling, this average time is considerably shorter and does not scale as  $1/L^2$ . We note that the critical value of global coupling is zero ( $\gamma_c=0$ ) in this system.

However, this short-time behavior is not universal. It depends on the nature of the map. We simulated CML for  $f(x)=x-x^n$ . This map has a marginally stable fixed point at  $x=0$ . We find that at  $\gamma=\gamma_c=0$ ,  $\epsilon \neq 0$ , we get a power-law decay of various order parameters. However,  $\alpha_1$ ,  $\alpha_2$ , and  $\alpha_3$  vary with  $n$ . We simulated this map for  $N=4000$ ,  $\gamma=0$ , and  $\epsilon=1$ . Figure 9(a) shows behavior of  $\sigma^2(N, t, 0)$  as a function of  $t$  for various values of  $n$ . It is clear that roughness decays slowly as one increases  $n$ . However, it still decays as a power law. In Fig. 9(b), we have plotted  $\alpha_3$  as a function of  $n$ . We observe that the exponent decays monotonically with  $n$ . Thus, exponents are not universal in synchronization of non-chaotic system.

## VI. PERSISTENCE IN COUPLED MAP LATTICES

In the past decade, persistence in spatially extended systems has been a matter of extensive study [36]. For spin systems, persistence at time  $t$  could simply be defined by counting the number of spins which did not flip *even once* during time evolution *until* time  $t$ . For dynamical systems,

there have been attempts to define persistence by coarse graining the system suitably. Menon *et al.* coarse grained the coupled circle maps by partitioning phase space points with reference to the fixed point [37]. After partitioning the system as above, they went on to define persistence in the same way as in spin systems. They just defined persistent sites at time  $t$  as those which were above (below) the fixed point at time  $t=0$  and did not attain value below (above) the fixed point at time  $t$ .

The reference point for departure from chaotic synchronization is obviously a synchronous state and not a fixed point. We know that in synchronous state, each space point has the same value as average; i.e.,  $x_i(t)=\langle x(t) \rangle$ . Thus, we compare with  $\langle x(t) \rangle$ . If we follow the prescription of Menon *et al.* entirely and define persistence  $P(t)$  by counting the fraction of sites that were above (below) the average and stayed above (below) average at all times till time  $t$ , it does not reflect transition to synchronization in any manner. Thus, it is necessary to modify it suitably so that it reflects the dynamic transition we are interested in. Now let us consider a situation in which one is considering the synchronized period-3 state. Natural definition would be to check if the spin values return to their old values after every three iterations. How can one extend this definition to a chaotic system? Since the system is chaotic, we do not know how it should behave. Hence, we impose some kind of self-consistency criterion. The generating partition is not known for the coupled system and we do not know how the system should evolve. We overcome this difficulty by defining persistent sites as those which have not departed from “normal” behavior. What is “normal?” Let us take a clue from sociology and define that whatever majority does is normal. We define sites which have values greater (less) than  $\langle x(0) \rangle$  initially as those with flag 1 (flag -1). These two groups are decided from the initial conditions at  $t=0$  and never mixed; i.e., sites with flag 1 never become -1 or vice versa. Now we do not know how these sites are supposed to behave. Thus, if at time  $t=1$  ma-

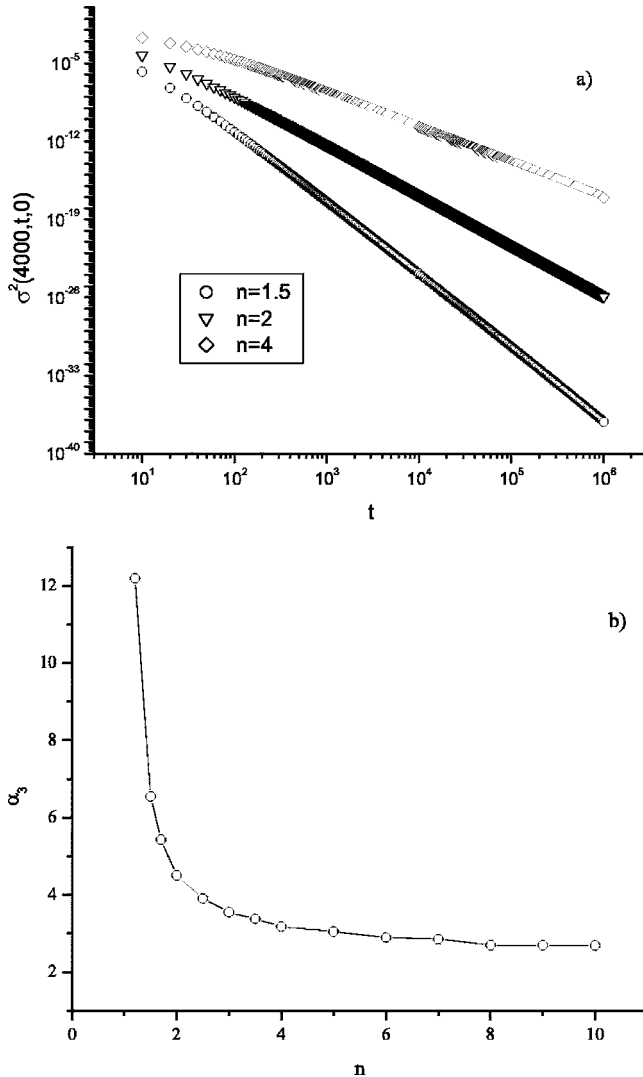


FIG. 9. (a) The quantity  $\sigma^2(4000, t, 0)$  is plotted as a function of  $t$  for  $f(x)-x-x^n$  for  $n=1.5$ ,  $n=2$ , and  $n=4$ . We average over 10 configurations. (b) Exponent  $\alpha_3$  is plotted as a function of  $n$  for the convergence to synchronous fixed point of the map  $f(x)=x-x^n$ .

jority of the sites with flag 1 have stayed above  $\langle x(1) \rangle$ , we will set the flag of minority sites as 0 and keep the flag of the rest of the sites unchanged. We check the same for sites with flag -1 to see if majority of them are above or below  $\langle x(1) \rangle$  and set the flag of minority sites to zero. We repeat this process and keep counting the number of persistent sites as sites which have a nonzero flag. In Fig. 10, we display an excellent power law at critical point over four decades with a critical exponent of 0.4. We have nonlocal interactions in the system and inferring about persistence from the behavior of all the sites seems to work well.

Unlike other exponents studied in the paper, persistence exponent does not seem to be universal. We found that exponent is around 0.3 for coupled logistic maps at  $\mu=4$ . This is not surprising since the persistence exponent is known to be far less universal than the other three exponents that typically characterize scaling behavior in interacting stochastic systems. The reason is that persistence probes the full, in general non-Markovian, time evolution of a local fluctuating

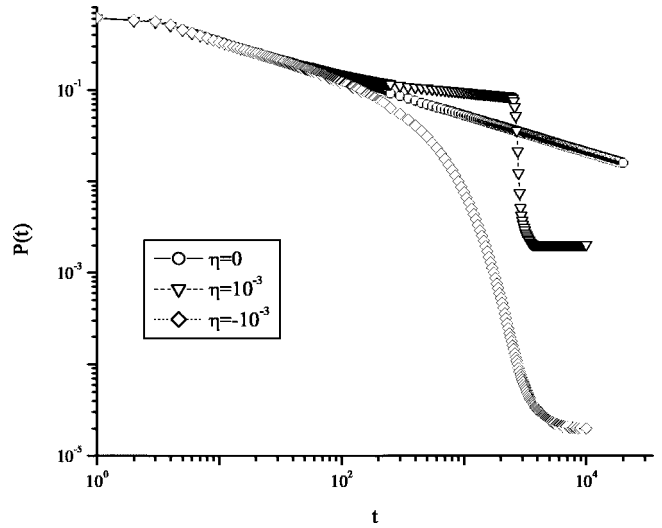


FIG. 10. Fraction of persistent sites  $P(t)$  as a function of  $t$  at various values of  $\eta$  for  $f(x)=G^3(x)$  with  $a=2$ ,  $\epsilon=0.1$ , and  $N=10^5$ . Averaging is done over 1000 configurations. We observe a clear power law at critical value of coupling  $\eta=0$ .

variable, such as a spin or density field, from its initial state [36]. We note here that Lemaître and Chaté also found that persistence exponent for phase ordering properties of lattices of band chaotic maps are not universal but vary with the value of coupling constant [38]. Swift and Bray also found that survival time distribution for an inelastic collapse shows power-law decay at long times with a nonuniversal exponent that depends on coefficient of restitution [39].

Obviously, there can be several possibilities for defining persistence in spatially extended system. If we follow the definition by Menon *et al.*, it does not reflect the transition to synchronization in chaotic systems while our definition shows a nice power-law decay at the critical point. It appears that the definition should be in accordance with the transition being investigated. Previous investigators have also defined it depending on the dynamic transition they are interested in. We feel our definition is well suited for describing transition to chaotic synchronization. Unfortunately, since we do not see previous instances where persistence is defined in a similar manner, it is difficult to have a meaningful comparison with other stochastic or dynamical transitions.

## VII. CONCLUSIONS

Finding critical exponents, determining universality class for dynamic phase transitions in spatially extended dynamical systems and comparing them with known transitions in stochastic systems is a relatively unexplored but interesting and important problem. Knowing that two apparently dissimilar problems fall in the same universality class helps us to identify the crucial factors that determine the critical behavior. In this work, we have drawn parallels between transition to synchronous chaos and directed percolation which is a nonequilibrium transition in stochastic systems. We studied the transition to synchronous chaos in coupled map

lattice with local-global and purely global couplings as a dynamic phase transition. We find that critical exponents for this transition in the presence of local-global coupling match with those of mean-field limit of directed percolation; i.e.,  $\alpha=\beta=1$  and  $z=2$ . For purely global couplings, the exponents are  $\alpha=\beta=1$  and  $z=0$ . The exponents  $\alpha$  and  $\beta$  are the same as for mean-field case, while reduction in  $z$  to zero is observed in case of directed percolation in the presence of long-range couplings in the limit of coupling decaying as  $1/r^d$  [34].

We note that long-range and nonlocal couplings are needed for the self-synchronization of all the elements of the same systems. We believe that the transition to synchronous

state, if continuous, should be generic irrespective of how the nonlocal field is incorporated, either by explicit mean-field or by small-world type connectivity or long-range correlations [5]. However, further studies are required to test this hypothesis.

P.M.G. thanks S. N. Majumdar for discussions and A. Nandgaonkar for carefully reading the manuscript. This work was supported by National Science Council in Taiwan under Grant Nos. NSC 93-2112-M 001-027 and NSC 94-2119-M-002-001, and Academia Sinica under Grant No. AS-91-TP-A02.

- 
- [1] H. E. Stanley, *Introduction to Phase Transitions and Critical Phenomena* (Oxford University Press, New York, 1971); L. P. Kadanoff, *Physica A* **163**, 1 (1990).
  - [2] C.-K. Hu, *Phys. Rev. B* **29**, 5103 (1984); F. Y. Wang and C.-K. Hu, *Phys. Rev. E* **56**, 2310 (1997); C.-K. Hu, C.-Y. Lin, and J.-A. Chen, *Phys. Rev. Lett.* **75**, 193 (1995); **75**, 2786(E) (1995); C.-K. Hu and C.-Y. Lin, *Phys. Rev. Lett.* **77**, 8 (1996).
  - [3] M. J. Feigenbaum, *J. Stat. Phys.* **19**, 25 (1978).
  - [4] See, for example, H. Hinrichsen, *Adv. Phys.* **49**, 815 (2000).
  - [5] See, for example, P. M. Gade and C.-K. Hu, *Phys. Rev. E* **60**, 4966 (1999); **62**, 6409 (2000), and references therein.
  - [6] I. Waller and R. Kapral, *Phys. Rev. A* **30**, 2047 (1984).
  - [7] K. Kaneko, *Prog. Theor. Phys.* **72**, 480 (1984); K. Kaneko, *Physica D* **34**, 1 (1989); **41**, 137 (1990); J. P. Crutchfield and K. Kaneko, *Phys. Rev. Lett.* **60**, 2715 (1988); K. Kaneko, *ibid.* **65**, 1391 (1990); see also *Theory and Applications of Coupled Map Lattices*, edited by K. Kaneko (Wiley, New York, 1993).
  - [8] D. Barkley, *Physica D* **49**, 61 (1991).
  - [9] W.-J. Ma, C.-K. Hu, and R. E. Amritkar, *Phys. Rev. E* **70**, 026101 (2004).
  - [10] See, for example, M. Barahona and L. M. Pecora, *Phys. Rev. Lett.* **89**, 054101 (2002).
  - [11] P. M. Gade and R. E. Amritkar, *Phys. Rev. E* **47**, 143 (1993).
  - [12] C. Anteneodo, S. E. de S. Pinto, A. M. Batista, and R. L. Viana, *Phys. Rev. E* **68**, 045202(R) (2003); C. Anteneodo, A. M. Batista, and R. L. Viana, *Phys. Lett. A* **326**, 227 (2004).
  - [13] S. Raghavachari and J. A. Glazier, *Phys. Rev. Lett.* **74**, 3297 (1995); W. Just, *Physica D* **81**, 317 (1995).
  - [14] See, e.g., D. Hansel and H. Sompolinsky, *J. Comput. Neurosci.* **3**, 7 (1996).
  - [15] W. J. Freeman, R. Kozma, and P. J. Werbos, *BioSystems* **59**, 109 (2001).
  - [16] P. L. Nunez, *Behav. Brain Sci.* **23**, 371 (2000); V. M. Eguluz, D. R. Chialvo, G. A. Ceochi, M. Baliki, and A. V. Apkarian, *Phys. Rev. Lett.* **94**, 018102 (2005).
  - [17] C. Tsallis, cond-mat/0010150 (2000).
  - [18] D. Bagtiktokh, *Phys. Rep.* **288**, 435 (1997).
  - [19] Z. Olami, B. Galanti, O. Kupervasser, and I. Procaccia, *Phys. Rev. E* **55**, 2649 (1997).
  - [20] Y. Kuramoto, D. Battogtokh, and H. Nakao, *Phys. Rev. Lett.* **81**, 3543 (1998); Y. Kuramoto, *Prog. Theor. Phys.* **94**, 321 (1995).
  - [21] A. Amengual, E. Hernandez-Garcia, R. Montagne, and M. SanMiguel, *Phys. Rev. Lett.* **78**, 4379 (1997).
  - [22] L. G. Morelli and D. H. Zanette, *Phys. Rev. E* **58**, R8 (1998).
  - [23] L. Baroni, R. Livi, and A. Torcini, *Phys. Rev. E* **63**, 036226 (2001); V. Ahlers and A. Pikovsky, *Phys. Rev. Lett.* **88**, 254101 (2002); M. A. Munoz and R. Pastor-Satorras, *ibid.* **90**, 204101 (2003).
  - [24] P. Grassberger, *Phys. Rev. E* **59**, R2520 (1999).
  - [25] M. Kardar, G. Parisi, and Y.-C. Zhang, *Phys. Rev. Lett.* **56**, 889 (1986).
  - [26] J. Rolf, T. Bohr, and M. H. Jensen, *Phys. Rev. E* **57**, R2503 (1998).
  - [27] See also P. Marcq, H. Chate, and P. Manneville, *Phys. Rev. Lett.* **77**, 4003 (1996).
  - [28] K. Y. Tsang and K. Wiesenfeld, *Appl. Phys. Lett.* **56**, 495 (1990).
  - [29] Very recently, there have been some works that try to explain the dynamical difference between continuous and discontinuous transitions. See, for example, M. Cencini and A. Torcini, *Physica D* **208**, 191 (2005); Z. Jabeen and N. Gupte, *Phys. Rev. E* **72**, 016202 (2005). F. Ginelli, H. Hinrichsen, R. Livi, D. Mukamel, and A. Politi [*Phys. Rev. E* **71**, 026121 (2005)] have studied the contact process with long-range interactions and found that the transition changes its nature from second order to first order when there are strong long-range interactions. However, we believe that analysis of dynamic phase transitions in the CML is more complicated and needs further study.
  - [30] J. Miller and D. A. Huse, *Phys. Rev. E* **48**, 2528 (1993).
  - [31] F. Xie and H. A. Cerdeira, *Phys. Rev. E* **54**, 3235 (1996).
  - [32] M. Hirsch and S. Smale, *Differential Equations, Dynamical Systems, and Linear Algebra* (Academic, New York, 1974), Chap. 5-2.
  - [33] S. Mukherji and S. M. Bhattacharjee, *Phys. Rev. Lett.* **79**, 2502 (1997).
  - [34] H. Hinrichsen and M. Howard, *Eur. Phys. J. B* **7**, 635 (1999).
  - [35] S. A. Cannas and F. A. Tamarit, *Phys. Rev. B* **54**, R12661 (1996).
  - [36] For a review, see S. N. Majumdar, *Curr. Sci.* **77**, 370 (1999).
  - [37] G. I. Menon, S. Sinha, and P. Ray, *Europhys. Lett.* **61**, 27 (2003); see also T. M. Janaki, S. Sinha, and N. Gupte, *Phys. Rev. E* **67**, 056218 (2003), in which other critical exponents for the same system have been obtained with high accuracy.
  - [38] A. Lemaître and H. Chaté, *Phys. Rev. Lett.* **82**, 1140 (1998).
  - [39] M. R. Swift and A. J. Bray, *Phys. Rev. E* **59**, R4721 (1999).